

Slow-Light Enhanced Spectrometers on Chip

Zhimin Shi^a, and Robert W. Boyd^{a,b}

^aThe Institute of Optics, University of Rochester, Rochester, New York 14627 USA;

^bDepartment of Physics, University of Ottawa, Ottawa ON K1N 6N5 Canada

ABSTRACT

We propose using slow light structures to greatly enhance the spectral performance of on-chip spectrometers. We design a calzone photonic crystal line-defect waveguide which can have large group index over a certain wavelength range. An arrayed waveguide gratings (AWGs) is studied as an example, and the performance of such a slow-light AWG is analyzed numerically.

Keywords: slow light, interferometer, photonic crystal

1. INTRODUCTION

Interferometric spectrometers are used in research and industry for a wide range of applications. The ability of an interferometric spectrometer to resolve closely spaced spectral components can prove extremely important for applications in analytic chemistry and biology. Meanwhile, integrated photonic devices are becoming more and more important because of their small footprints and easy integration of various functional modules to form various types of systems-on-a-chip. Thus, a miniaturized spectrometer with unprecedented spectral performance becomes desirable and can lead to molecular and biological substance recognition on a chip.

Slow- and fast-light technology¹ has recently attracted a great deal of interest, both in terms of fundamental and practical aspects.²⁻⁶ It has recently been shown that slow light can be used to enhance the performance of various types of spectroscopic interferometers.⁷⁻¹¹ It has also been recently shown that by changing the width of a channel waveguide, one can enhance the group index by a factor of approximately 30%, which can be used for integrated dispersive elements such as arrayed waveguide gratings.¹²

In this work, we study the use of slow light to build on-chip miniaturized spectroscopic interferometers with very high spectral sensitivity or resolution. We first propose a new type of slow-light waveguide based on calzone photonic crystal (PhC) W1 line-defect waveguide structures. We show that by optimizing the geometry of our calzone PhC W1 waveguide, one can achieve uniform and large group index over a certain wavelength range. We further illustrate the performance of various types of on-chip spectroscopic interferometers, including an arrayed waveguide grating, incorporated with our slow-light medium.

2. DESIGN OF A FLAT-BAND SLOW-LIGHT CALZONE PHOTONIC CRYSTAL WAVEGUIDE

An on-chip slow-light medium that is suitable for spectroscopic applications has to meet a number of criteria,¹³ including a large wavelength range over which the group index maintains approximately constant, and a large ratio between the group index and associate loss .

Among other types on-chip slow-light mechanisms, photonic bandgap structures are very promising on-chip slow light mechanisms,¹⁴⁻¹⁹ and have been used for on-chip delay lines as well as for nonlinear optical processing. In this work, we propose a new geometry of a flat-band, slow-light photonic crystal line-defect waveguide. Our geometry is based on a hexagonal lattice W1 line defect waveguide, in which one row of holes is removed to serve as the core of the waveguide. Besides that, the first rows on each side of the defect line are truncated into semicircles. Due to the shape of the first rows, we name our proposed structure “a calzone line-defect waveguide” following Ref.²⁰ A schematic diagram of the waveguide structure is plotted in Fig. 1. The design parameters include the width of the line defect w , the radius of the holes r , and the lattice constant a .

As an example, we choose the parameters $a = 403$ nm, $r = 0.3$, and $w = 0.7 \times \sqrt{3}a = 488.6$ nm. Planewave expansion analysis²¹ is used to calculate the dispersion relation, the calculation result over the wavelength range

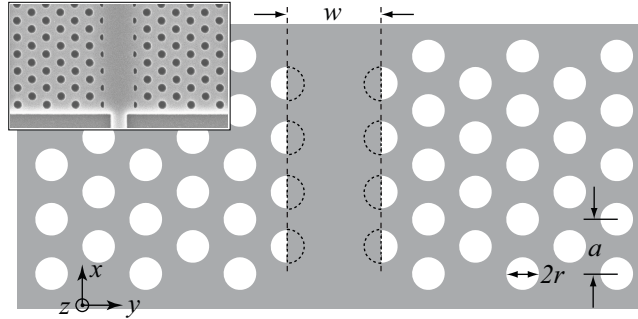


Figure 1. Two-dimensional schematics of a slab photonic crystal calzone line-defect waveguide with lattice constant a and hole radius r . The inset shows a scanning microscope micrograph of a fabricated calzone PhC waveguide.

near 1550 nm is shown in Fig. 2(a). The corresponding effective mode index n_{eff} and reduced group index n'_g as functions of wavelength are plotted in Fig. 2(b) and (c), respectively. One sees that for this design, there is a plateau near $\lambda = 1551$ nm over which the group index is approximately 60. If one defines the working bandwidth by requiring that the group index does not change by more than 10% within the bandwidth, this example calzone waveguide structure has a working bandwidth of 3.2 nm.

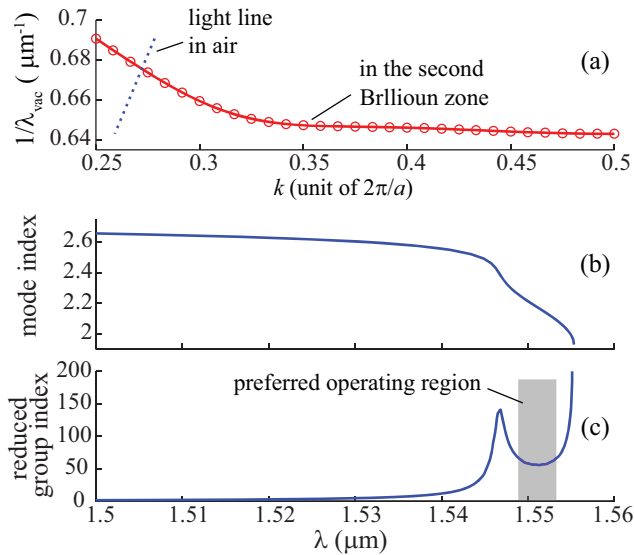


Figure 2. (a) dispersion relations of the fundamental guided Bloch modes of a flat-band calzone line-defect waveguide with $a = 403$ nm, $r = 0.3$, and $w = 488.6$ nm; corresponding effective mode index (b) and reduced group index n'_g (c) as functions of wavelength for such a waveguide structure.

We have also analyzed the effect of any changes of the values of r and w on the mode dispersion. Generally speaking, an increasing r leads to a higher but narrower group index plateau with a shift towards shorter wavelengths. Meanwhile, as w increases, on the other hand, the group index plateau shifts towards longer wavelengths (lower frequency), and the height of the plateau decreases while its width increases. With optimizing other geometrical parameters of the waveguide structure, one can possibly further increase the group index of the waveguide with an adequate bandwidth over a few nanometers.

3. DESIGN OF THE GEOMETRY OF AN ON-CHIP SPECTROMETER

There are many different geometries that can be applied to construct an on-chip spectrometer, such as Mach-Zehnder interferometer, etched diffraction grating,^{22,23} arrayed waveguide grating,²⁴ and so on. Here, we study the case of an arrayed waveguide grating (AWG) as an illustrating example.

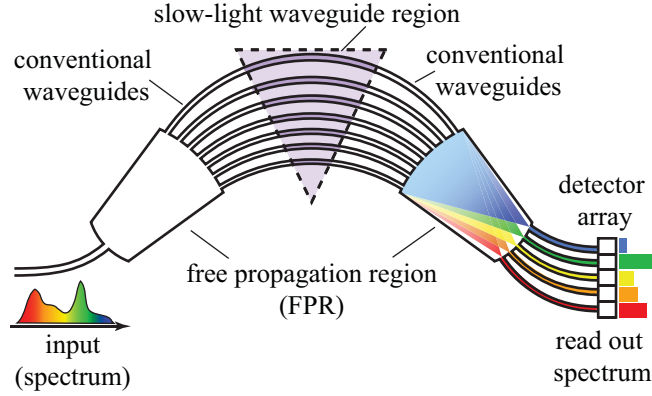


Figure 3. Schematic diagram of a slow-light arrayed waveguide grating spectrometer.

A conventional AWG is typically comprised of three parts as shown in Fig. 3. The input signal field first propagates through a free-propagation region (FPR) to expand its beam width. The field is then coupled into a series of waveguides. The waveguides are designed such that the lengths of neighboring waveguides differ by a fixed amount $\Delta l = m\lambda_0/n_{\text{eff}}$ where λ_0 is the designed central (vacuum) wavelength of the device, and n_{eff} is the effective refractive index (i.e., mode index) of the waveguides. The output ports of these waveguides are spaced periodically (with a period of Λ) at the entrance to a second FPR, and the fields exiting from the waveguides array will constructively interfere and focus at the other side of the second FPR. The diffraction equation of such an AWG is given by

$$n_{\text{wg}}\Delta l + n_{\text{FPR}}\Lambda(\sin\theta_{\text{inc}} + \sin\theta_{\text{diff},m}) = m\lambda, \quad (1)$$

where n_{wg} and n_{FPR} are the effective mode indices for the waveguides and the FPR, respectively.

When the dispersion of n_{wg} and n_{FPR} are negligible, the angular dispersion of such an AWG is given by

$$\frac{d\theta_{\text{diff},m}}{d\lambda} = \frac{m}{n_{\text{eff}}\Lambda \cos\theta_{\text{diff},m}} \quad (2)$$

Since m is independent of Λ in this case, an AWG can, in principle, can have arbitrarily large angular dispersion. However, a large angular dispersion indicates that Δl must be large, which leads to an increased footprint of the device.

If the dispersion of n_{wg} and n_{FPR} are taken into account, the diffraction equation becomes modified as follows:

$$\begin{aligned} \frac{d\theta_{\text{diff},m}}{d\lambda} &= \frac{mn_{g,\text{FPR}}}{n_{\text{FPR}}^2\Lambda \cos\theta_{\text{diff},m}} - \frac{\Delta l}{n_{\text{FPR}}\Lambda \cos\theta_{\text{diff},m}} \frac{dn_{\text{wg}}}{d\lambda} \\ &\quad + \frac{n_{\text{wg}}\Delta l}{n_{\text{FPR}}^2\Lambda \cos\theta_{\text{diff},m}} \frac{dn_{\text{FPR}}}{d\lambda} \\ &= \frac{mn_{g,\text{FPR}}}{n_{\text{FPR}}^2\Lambda \cos\theta_{\text{diff},m}} \\ &\quad + \frac{n_{\text{wg}}\Delta l}{n_{\text{FPR}}\lambda\Lambda \cos\theta_{\text{diff},m}} \left(\frac{n'_{g,\text{wg}}}{n_{\text{wg}}} - \frac{n'_{g,\text{FPR}}}{n_{\text{FPR}}} \right). \end{aligned} \quad (3)$$

Here, we consider the case in which the waveguide has large modal dispersion (i.e., large dispersion on the effective index), but the dispersion of the FPR is negligible. In such a case, the angular dispersion becomes

$$\begin{aligned} \frac{d\theta_{\text{diff},m}}{d\lambda} &= \frac{m}{n_{\text{FPR}}\Lambda \cos\theta_{\text{diff},m}} \\ &\quad + \frac{n'_{g,\text{wg}}\Delta l}{n_{\text{FPR}}\lambda\Lambda \cos\theta_{\text{diff},m}}. \end{aligned} \quad (4)$$

One sees that in such a case, the angular dispersion of the AWG comes from two contributions, one containing the non-slow-light contribution and one containing the slow-light contribution from the waveguide.

In practice, an AWG can work in a configuration such that the diffraction angle for the central wavelength is zero degree to minimize the influence of aberrations, etc. In such cases, the diffraction order m of the AWG depends primarily on the waveguide increment Δl such that $m \approx n_{wg} \Delta l / \lambda$, and the angular dispersion is given by

$$\frac{d\theta_{\text{diff},m}}{d\lambda} \approx \frac{n_{g,\text{wg}} \Delta l}{n_{\text{FPR}} \lambda \Lambda \cos \theta_{\text{diff},m}} \quad (5)$$

$$= \frac{n_{g,\text{wg}} m}{n_{\text{FPR}} n_{\text{wg}} \Lambda \cos \theta_{\text{diff},m}}. \quad (6)$$

One sees that by using a slow-light waveguide array, the angular dispersion of an AWG can be enhanced by a factor of $n_{g,\text{wg}}/n_{\text{wg}}$, and therefore one can enhance the spectral resolution by the same factor.

Here, we demonstrate our design using a numerical example based on the Silicon-On-Insulator (SOI) platform. We assume the center wavelength to be $1.55 \mu\text{m}$. The refractive indices for Si and SiO_2 are $n_{\text{Si}} = 3.476$ and $n_{\text{SiO}_2} = 1.5$, respectively. We assume the spacing between the output of neighboring waveguides to be $3 \mu\text{m}$, the diffraction angle $\theta_{\text{diff}} = 0^\circ$ at the center wavelength, and the length of the FPR to be $R_{\text{FPR}} 1.5 \text{ mm}$.

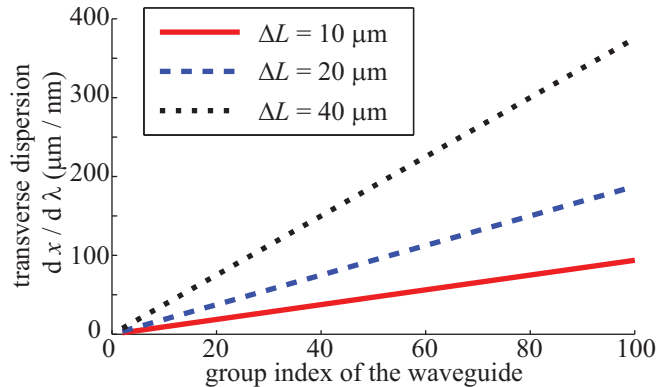


Figure 4. Linear transverse dispersion at the focal plane of the output FPR as a function of the group index of the waveguide of a slow-light AWG with $\Delta L = 10, 20$ and $40 \mu\text{m}$, respectively.

Figure.4 shows the calculated transverse dispersion at the focal plane of the output FPR of a slow-light AWG as a function of the group index $n_{g,\text{wg}}$ of the waveguides. Here the transverse dispersion $dx/d\lambda = R_{\text{FSR}} d\theta_{\text{diff},m}/d\lambda$, where the angular dispersion $d\theta_{\text{diff},m}/d\lambda$ is given by Eq. 5. When the $n_{g,\text{wg}} = 3$ and $\Delta L = 10 \mu\text{m}$, the transverse dispersion is approximately $2.8 \mu\text{m}/\text{nm}$, which is just adequate to separate two wavelength differing 1 nm as two spectral channels in a wavelength division multiplexing system. When $n_{g,\text{wg}} = 100$, the transverse dispersion increases to $94 \mu\text{m}/\text{nm}$. If we let $\Delta L = 40 \mu\text{m}$, the transverse dispersion is $375 \mu\text{m}/\text{nm}$. If the distance between neighboring output waveguide is $3 \mu\text{m}$, this indicates a spectral resolution of 1 GHz . Note that the group index in photonic crystal waveguides can be as large as $230^{16,25}$ or even more, which indicates the possibility of a further increase in the spectral resolution.

4. SUMMARY

We have proposed building on-chip spectroscopic interferometers using calzone photonic crystal line-defect waveguides. By optimizing its geometrical parameters, we have shown that such a waveguide can have a large group index over a certain wavelength range, and therefore is suitable to be used in on-chip spectroscopic interferometers. We have also analyzed the potentials of on-chip slow-light spectroscopic interferometers using an arrayed waveguide grating as an example. Our numerical simulation shows that spectral resolution of the order of GHz can be achieved, and therefore our approach opens the possibility of on-chip system for chemical and biological substance recognition.

ACKNOWLEDGMENTS

This project received support from the Defense Threat Reduction Agency-Joint Science and Technology Office for Chemical and Biological Defense (grant no. HDTRA1-10-1-0025). This work was performed in part at the Cornell NanoScale Facility, a member of the National Nanotechnology Infrastructure Network, which is supported by the National Science Foundation (Grant ECS-0335765).

REFERENCES

- [1] Boyd, R. W. and Gauthier, D. J., “‘Slow’ and ‘fast’ light,” in [*Progress in Optics*], Wolf, E., ed., **43**, 497–530, Elsevier Science, Amsterdam (2002).
- [2] Chang-Hasnain, C. J. and Chuang, S. L., “Slow and fast light in semiconductor quantum-well and quantum-dot devices,” *J. Lightwave Technol.* **24**(12), 4642–4654 (2006).
- [3] Milonni, P. W., [*Fast light, slow light and left-handed light*], Institute of Physics, Bristol and Philadelphia (2005).
- [4] Milonni, P. W., “Controlling the speed of light pulses,” *Journal of Physics B: Atomic, Molecular and Optical Physics* **35**(6), R31 (2002).
- [5] Khurgin, J. B., “Slow light in various media: a tutorial,” *Adv. Opt. Photon.* **2**(3), 287–318 (2010).
- [6] Boyd, R. W., “Slow and fast light: Fundamentals and applications,” *J. Mod. Opt.* **56**(18), 1980–1915 (2009).
- [7] Shahriar, S. M., Pati, G., Gopal, V., Tripathi, R., Cardoso, G., Pradhan, P., Messal, M., and Nair, R., “Precision rotation sensing and interferometry using slow light,” in [*Quantum Electronics and Laser Science Conference (QELS)*], (paper JWB97, 2005).
- [8] Shi, Z., Boyd, R. W., Gauthier, D. J., and Dudley, C. C., “Enhancing the spectral sensitivity of interferometers using slow-light media,” *Opt. Lett.* **32**(8), 915–917 (2007).
- [9] Pati, G. S., Salit, M., Salit, K., and Shahriar, M. S., “Demonstration of a tunable-bandwidth white-light interferometer using anomalous dispersion in atomic vapor,” *Physical Review Letters* **99**(13), 133601 (2007).
- [10] Shi, Z., Boyd, R. W., Camacho, R. M., Vudyasētu, P. K., and Howell, J. C., “Slow-light Fourier transform interferometer,” *Phys. Rev. Lett.* **99**(24), 240801 (2007).
- [11] Bortolozzo, U., Residori, S., and Huignard, J.-P., “Slow-light birefringence and polarization interferometry,” *Opt. Lett.* **35**, 2076–2078 (Jun 2010).
- [12] Matos, O., Calvo, M., Cheben, P., Janz, S., Rodrigo, J., Xu, D.-X., and Delage, A., “Arrayed waveguide grating based on group-index modification,” *Lightwave Technology, Journal of* **24**, 1551–1557 (march 2006).
- [13] Shi, Z. and Boyd, R. W., “Slow-light interferometry: practical limitations to spectroscopic performance,” *J. Opt. Soc. Amer. B* **25**(12), C136–C143 (2008).
- [14] Soljačić, M., Johnson, S. G., Fan, S., Ibanescu, M., Ippen, E., and Joannopoulos, J. D., “Photonic-crystal slow-light enhancement of nonlinear phase sensitivity,” *J. Opt. Soc. Amer. B* **19**, 2052–2059 (Sep 2002).
- [15] Gersen, H., Karle, T. J., Engelen, R. J. P., Bogaerts, W., Korterik, J. P., van Hulst, N. F., Krauss, T. F., and Kuipers, L., “Real-space observation of ultraslow light in photonic crystal waveguides,” *Phys. Rev. Lett.* **94**, 073903 (Feb 2005).
- [16] Vlasov, Y. A., O’Boyle, M., Hamann, H. F., and McNab, S. J., “Active control of slow light on a chip with photonic crystal waveguides,” *Nature* **438**(3), 65–69 (2005).
- [17] Krauss, T. F., “Slow light in photonic crystal waveguides,” *J. of Physics D: Applied Physics* **40**(9), 2666–2670 (2007).
- [18] Baba, T., “Slow light in photonics crystals,” *Nature Photonics* **2**, 465–473 (2008).
- [19] Anderson, S. P., Shroff, A. R., and Fauchet, P. M., “Slow light with photonic crystals for on-chip optical interconnects,” *Advances in Opt. Technol.* **2008**, 293531 (2008).
- [20] Hennessy, K., Hogerle, C., Hu, E., Badolato, A., and Imamoglu, A., “Tuning photonic nanocavities by atomic force microscope nano-oxidation,” *Appl. Phys. Lett.* **89**(4), 041118 (2006).
- [21] Johnson, S. G. and Joannopoulos, J. D., “Block-iterative frequency-domain methods for Maxwell’s equations in a planewave basis,” *Opt. Express* **8**(3), 173–190 (2001).

- [22] He, J.-J., Lamontagne, B., Delage, A., Erickson, L., Davies, M., and Koteles, E., "Monolithic integrated wavelength demultiplexer based on a waveguide rowland circle grating in ingaasp/lnp," *Lightwave Technology, Journal of* **16**, 631–638 (apr 1998).
- [23] Janz, S., Balakrishnan, A., Charbonneau, S., Cheben, P., Cloutier, M., Delage, A., Dossou, K., Erickson, L., Gao, M., Krug, P., Lamontagne, B., Packirisamy, M., Pearson, M., and Xu, D.-X., "Planar waveguide echelle gratings in silica-on-silicon," *Photonics Technology Letters, IEEE* **16**, 503–505 (feb. 2004).
- [24] Smit, M. and Van Dam, C., "Phasar-based wdm-devices: Principles, design and applications," *IEEE J. Sel. Topics Quantum Electron.* **2**, 236–250 (jun 1996).
- [25] Jacobsen, R., Lavrinenko, A., Frandsen, L., Peucheret, C., Zsigri, B., Moulin, G., Fage-Pedersen, J., and Borel, P., "Direct experimental and numerical determination of extremely high group indices in photonic crystal waveguides," *Opt. Express* **13**(20), 7861–7871 (2005).